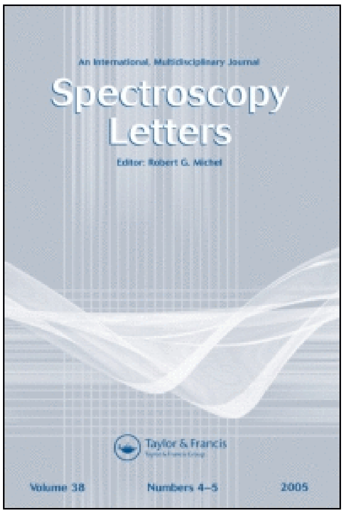

Spectroscopy Letters
Publication details, including instructions for authors and subscription information:
http://www.informaworld.com/smpp/title~content=t713597299

Interference Effects from Easily Ionizable Elements in Flame AES and ICP-OES: A Proposed Simplified Rate Model Based on Collisional Charge Transfer Between Analyte and Interferent Species

Mark F. Zaranyika[a]; Albert T. Chirenje[a]; Courtie Mahamadi[b]
[a] Chemistry Department, University of Zimbabwe, Mount Pleasan, Harare, Zimbabwe [b] Chemistry Department, Bindura University of Science Education (BUSE), Bindura, Zimbabwe

To cite this Article Zaranyika, Mark F. , Chirenje, Albert T. and Mahamadi, Courtie(2007) 'Interference Effects from Easily Ionizable Elements in Flame AES and ICP-OES: A Proposed Simplified Rate Model Based on Collisional Charge Transfer Between Analyte and Interferent Species', Spectroscopy Letters, 40: 6, 835 — 850

To link to this Article: DOI: 10.1080/00387010701436455

URL: http://dx.doi.org/10.1080/00387010701436455

Spectroscopy Letters, 40: 835–850, 2007

ISSN 0038-7010 print/1532-2289 online
DOI: 10.1080/00387010701436455

Interference Effects from Easily Ionizable Elements in Flame AES and ICP-OES: A Proposed Simplified Rate Model Based on Collisional Charge Transfer Between Analyte and Interferent Species

Mark F. Zaranyika and Albert T. Chirenje
Chemistry Department, University of Zimbabwe, Mount Pleasan, Harare,
Zimbabwe

Courtie Mahamadi
Chemistry Department, Bindura University of Science Education
(BUSE), Bindura, Zimbabwe

Abstract: The effects of excess Na and K on K and Mg atom line emission in the air-acetylene flame and of excess Li and K on Ca, Mg, and Sr atom and ion lines in inductively coupled plasma spectroscopy were studied using emission signal ratios, I'/I as probes, where I' and I are the emission readings in the presence and absence of the interferent respectively. The I'/I plots as a function of analyte concentration in the test solution for the ICP experiments were similar to those obtained for the flame experiments in the analytical range 0–10 mg/L. A simplified rate model based on analyte excitation via charge transfer between analyte ions and activated interferent atoms is proposed to account for the emission signal enhancement observed at low analyte concentrations (<1 mg/L) for both ICP-AES and flame atomic emission spectroscopy (AES). Data are presented showing good agreement between experimental E' calibration curves and theoretical E' calibration curves computed using the simplified rate model.

Keywords: Calibration curve, collisional charge transfer, easily ionizable element, flame AES, ICP-AES, simplified rate model

Received 4 September 2006, Accepted 23 April 2007

Address correspondence to Courtie Mahamadi, Chemistry Department, Bindura University of Science Education (BUSE), Postal Bag 1020, Bindura, Zimbabwe. E-mail: courtiema@yahoo.com

INTRODUCTION

Inductively coupled plasma spectroscopy (ICP) is relatively free from interferences and is easily coupled to mass spectrometry. However, although ICP has been around for about 30 years, mechanisms of analyte excitation and ionization are not fully understood. The result is that those matrix interferences that do exist cannot be explained easily.[1] Characteristically, easily ionized elements (EIEs) can cause enhancement or depression of the analyte emission signal.

Several workers have studied interference effects from easily ionized elements in ICP[2–8] and flame atomic emission spectrometry (AES).[9,10] Mechanisms that have been proposed to explain the effects of easily ionizable elements include shifts in the ionization equilibrium,[2–4] enhanced collisional excitation,[2,4,5] volatilization effects,[2,4] ambipolar diffusion,[2,4] and nebulizer effects,[2] quenching of Ar metastable atoms,[7–10] charge transfer involving Ar species,[11] radiation trapping with population of resonant levels of Ar,[12–14] direct electron impact ionization and excitation,[15] and autoionization and dielectric recombination.[16,17] In spite of this huge volume of work, there is still no agreement on the dominant mechanism.[18,19]

The classic collisional-radiative rate model approach takes into account all possible electronic states of the analyte and matrix. The major problem associated with this classic approach lies in the complexity of the models such that arriving at solutions is difficult. In previous work,[20,21] we proposed a simplified model that focuses on only one particular electronic level. Along with the simplified model, we proposed a novel method for probing changes in the number density of the analyte excited state, n_u, based on determining the analyte emission (I) signal ratio I'/I, where the prime denotes presence of interferent, and comparing with theoretical values derived assuming a simplified rate model based on steady-state kinetics in the plasma. The approach assumes no change in the rate of introduction of analyte atoms and no change in the temperature of the torch or flame upon the simultaneous introduction of an easily ionized interferent element. Under these conditions, it can be shown that $I'/I = 1$, provided there are no collisional effects resulting from the presence of the interferent. If there are collisional effects resulting from the presence of the interferent, then $I'/I \neq 1$.

The effects of EIEs on analyte line emission are observed in flame atomic spectrometry, as well as in ICP-OES (optical emission spectroscopy).[2] The aims of the current work were therefore to conduct a comparative study of the effects of EIEs on analyte line emission intensity during ICP-OES and air-acetylene flame AES, with a view to identifying any differences in the results obtained that might be attributed to the difference in composition and temperature of the plasma involved. This was achieved by measuring the line emission intensities of a range of analyte concentrations in the absence and presence of a fixed interferent concentration and noting how and to what extent the values of I'/I obtained deviate from unity.

MATERIALS AND METHODS

ICP Equipment

A Unicam 701-Emission Inductively Coupled Argon Plasma Echelle Spectrophotometer (Japan) with "crossed" dispersion was used. The spectrophotometer was fitted with an aperture plate of 90 mm by 1.5 nm slits etched at 2-mm intervals; a photomultiplier tube (PMT) detector mounted on a movable frame for radial view of the ICP; a torch with three concentric tubes for outer gas, auxiliary gas, and sample transport; a 40.68-MHz radiofreguency generator that supplies power up to 2 kW; a grid-type nebulizer fitted with Pt screens and Pt orifice; a 5-channel computer-controlled peristaltic pump; and an automatic Ar gas flow rate optimizer.

The argon (99.95%) was supplied from a pressurized tank (BOC GAS Ltd, Harare, Zimbabwe): The outer gas was supplied at 14 L min^{-1}, power 1.0 kW, nebulizer pressure 40 psi (280 KPa), and auxiliary gas at 1 L min^{-1}. Under these conditions, the excitation temperature is between 7000 K and 9000 K.[22] Mg(II), Ca(II), and Sr(II) line emission signals were recorded at 279.6, 393.3, and 407.8 nm respectively. The instrument was optimized using a 100 mg/L solution of Mn. The strong emission of Mn line was used to find the optimum zone for analysis. The maximum temperature of 9000 K was used in the calculations for maximum effect of the interferent.

Flame Equipment

Flame experiments were run using a Shimadzu AA–6701 Flame Atomic Absorption/Emission Spectrometer fitted with a high-resolution Czerny-Turner monochromator (Japan), automatic baseline drift correction using electrical double-beam signal processing, an air-cooled premix type 100-mm single-slot burner with a stainless steel head, Pt-Ir capillary nebulizer with Teflon orifice, glass impact bead, and polypropylene chamber. The spectrometer was coupled to an ASC-6100 Shimadzu Auto Sampler. The air was supplied by an Atlas Copco air compressor (ETS SESCA, France) at 350 KPa input pressure, and the fuel gas, acetylene, was supplied from a pressurized tank (Oxyco Zimbabwe, Harare, Zimbabwe) at 1000 kPa. The spectrophotometer was fitted with an automatic fuel gas flow rate optimization for each element to be measured. Optimum air-acetylene gas flow rates for K and Mg were 2.0 and 1.8 L/min. Under these conditions, the temperature of the flame is 2300°C (Shimadzu AA 6701 user manual). Other instrumental settings employed were as follows: wavelength 766.5 nm and 285.2 nm for K and Mg, respectively; slit width 0.1 nm; burner height 7 mm; burner angle 0°; secondary acetylene gas pressure 90 kPa, pre-spray time 3 s, integration time 5 s; and response time 1 s.

Materials

The following materials were used: calcium chloride, magnesium chloride, strontium chloride, lithium chloride, potassium chloride, and sodium chloride, all AR grade; de-ionized water of conductivity 0.002 μS.

Procedure

Two sets of standard solutions containing 0 to 30 mg/L analyte (Ca, Mg, Sr, or K) were prepared from freshly prepared solutions of their chloride salt solutions. One set was spiked with 1000 mg/L of interferent (Li, K, or Na) also prepared from the chloride salt. The other set was left unspiked. In order to minimize changes in the physical properties of the test solution upon the introduction of the interferent, the interferent concentration was kept constant at a very high level (1000 mg/L) relative to that of the analyte (0–30 mg/L), whereas the analyte concentration was varied. Under these conditions, any effect due the to changes in the physical properties of the test solution in going from the interferent-free solution to the interferent-spiked solution would affect the series of interferent-spiked solutions to the same extent, and this can be compensated for by taking blank readings of a solution containing the interferent salt only (Figure 1).

Readings were made in triplicate and corrected for the blank readings; the ratios I'/I calculated and plotted as a function of the analyte concentration in test solution in Figs. 2–4. Preliminary experiments were run to determine the aspiration rate and the nebulization efficiency for the type of solutions under analysis.[20] Mean values obtained for the aspiration rate and nebulization efficiency were 1.00 ± 0.04 and 5.0 ± 0.7% (n = 8), respectively, for the ICP experiments and 4.0 ± 0.1 g/min(h = 8 and n = 20) and 5.7 ± 0.2% (h = 12 and n = 1), respectively, for the flame experiments, where h = number of samples and n = number of replicates.

Theoretical Calculations

The rate constant for thermal excitation, k_Δ, was calculated using the equation

$$k_\Delta = (g_u/g_o)\exp(-\Delta E/kT), \tag{1}$$

where g_u and g_o are the statistical weights of the excited and ground states, respectively, ΔE is the energy difference between the two states, k is the Boltzmann constant, and T is the absolute temperature. The values of k_Δ obtained for Ca(II), Mg(II), and Sr(II) in the ICP ($T = 9000$ K) are shown in Table 1.

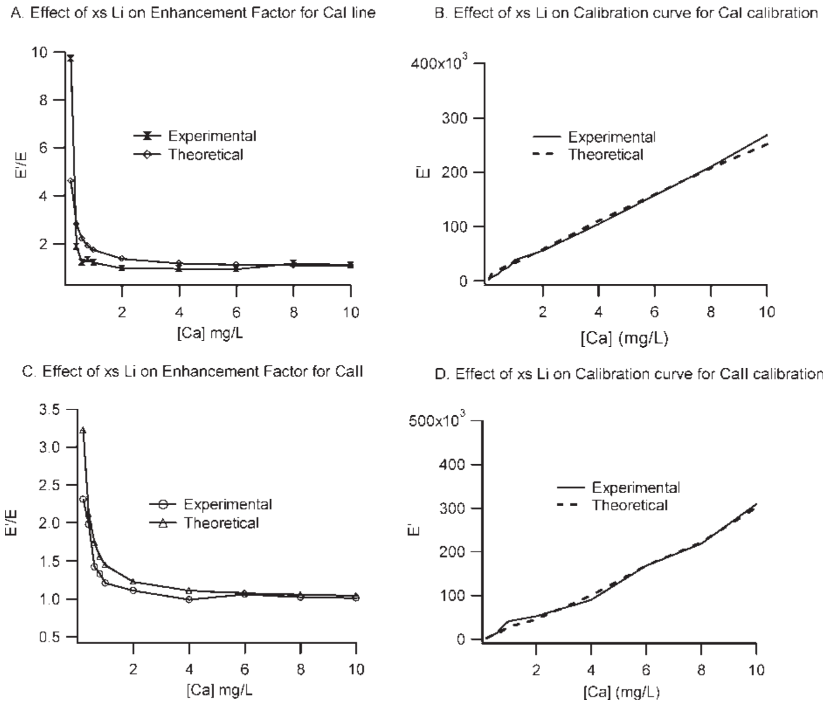
A. Effect of xs Li on Enhancement Factor for CaI line

B. Effect of xs Li on Calibration curve for CaI calibration

C. Effect of xs Li on Enhancement Factor for CaII

D. Effect of xs Li on Calibration curve for CaII calibration

Figure 1. Effect of 1000 mg/L Li on Ca atom and ion line emission intensity.

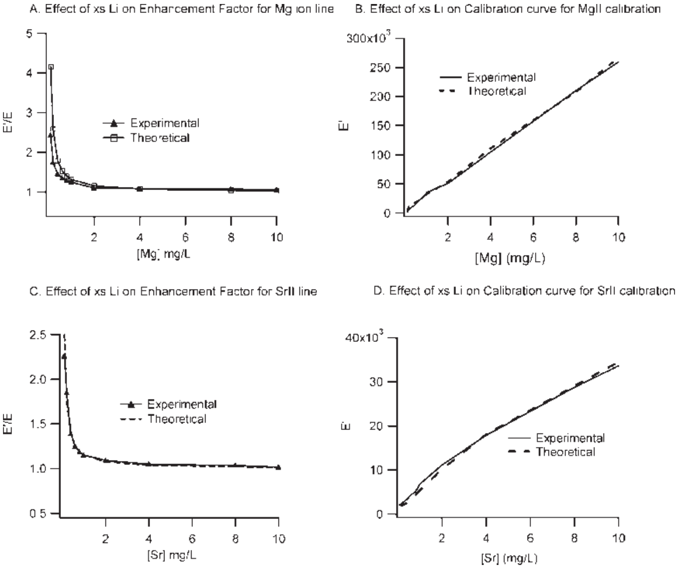
A. Effect of xs Li on Enhancement Factor for Mg ion line

B. Effect of xs Li on Calibration curve for MgII calibration

C. Effect of xs Li on Enhancement Factor for SrII line

D. Effect of xs Li on Calibration curve for SrII calibration

Figure 2. Effect of 1000 mg/L Li on Mg and Sr ion line emission intensity and calibration curves in the ICAP.

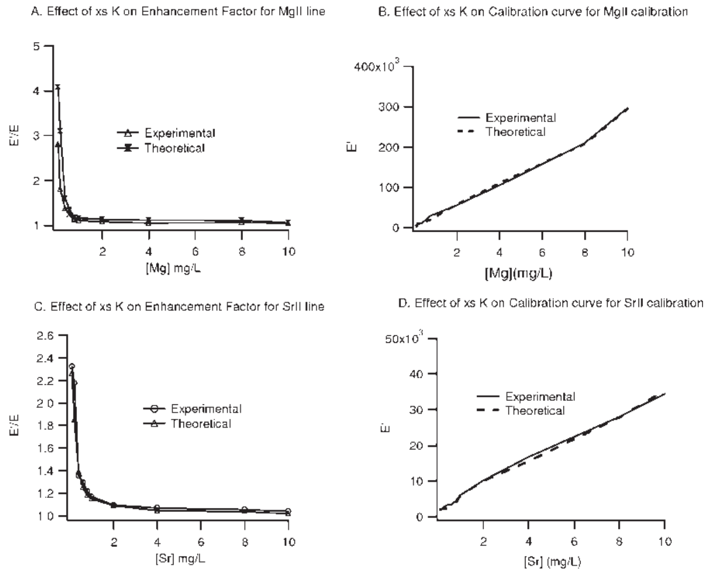

Figure 3. Effect of 1000 mg/L K on Mg and Sr ion line emission intensity and calibration curves in the ICP.

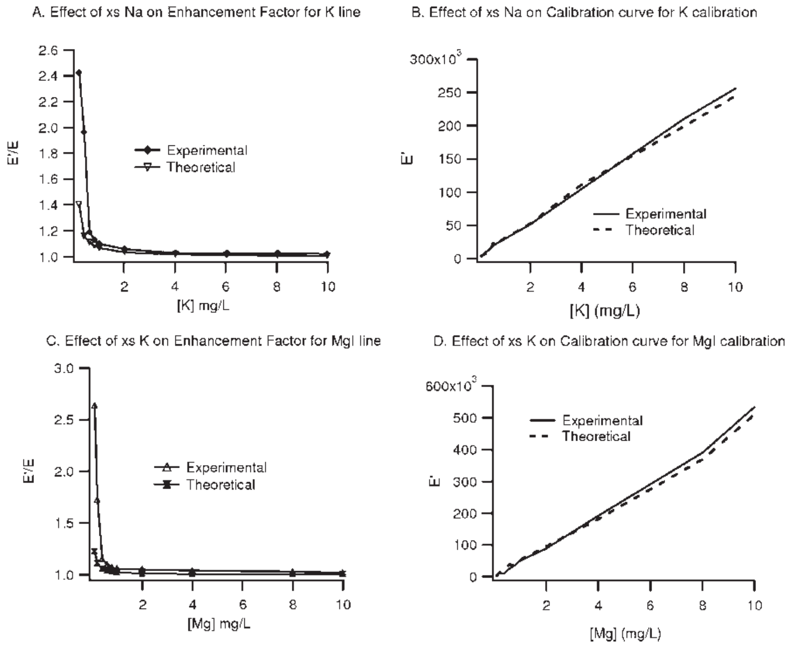

Figure. 4. Effect of 1000 mg/L Na on K line emission and 1000 mg/L K on MgI line emission in the air-acetylene flame.

Table 1. Values of ΔE, k_Δ and k_{hv} for Ca(II), Mg(II), Sr(II), and K

M	ΔE (eV)	g_{u}	g_{o}	k_Δ	k_{hv}
ICP experiments					
CaI	2.933	3	1	2.2781e-2	3.7312e + 8
CaII	3.152	4	2	3.4341e-2	4.3098e + 8
MgII	4.435	4	2	6.5702e-3	8.531e + 8
SrII	4.042	4	2	3.9671e-2	4.0095e + 8
Air-acetylene experiments					
K	1.618	4	2	6.7865e-4	1.1348e + 8
Mg	4.351	4	2	2.3942e-4	1.4821e + 8

Flame and ICP temperatures were 2573 K and 9000 K, respectively.

The rate constants for radiative relaxation, $k_{h_\nu}(\psi^2 \to \psi^1)$, is given by:[23]

$$k_{h_\nu(\psi^2\to\psi^1)} = (\sigma_{\max})^2 f/1.5, \tag{2}$$

where $\sigma_{\max}$ is the wavenumber for the maximum wavelength, λ, of the emission, and $f \approx 1$, where f is the oscillator strength. The values of $k_{h\nu}$ obtained are shown in Table 1.

Calculation of Flow Number Densities

For the ICP experiments, flow number densities were calculated assuming 1.00 $\pm$ 0.04 mL/min aspiration rate and 5.0 $\pm$ 0.7% nebulization efficiency and 9000 K temperature. The number density of metal species in the plasmas (e.g., for Ca species) is a product of {mass of Ca aspirated by nebulizer $\times$ nebulization efficiency $\times$ conversion factor from mass to mole for Ca $\times$ Avogadro's number $\times$ carrier gas volumetric flow rate $\times$ expansion factor of carrier gas from room temperature to the plasma temperature, that is,

$$\begin{aligned}
&\mathrm{c\,(mg)Ca/L} \times 5\% \times \frac{1\ \mathrm{mole}}{40\ \mathrm{g\,Ca}} \times 6.02 \times 10^{23}/\mathrm{mole}\\
&\times \frac{1}{1\ \mathrm{L\,Ar/\,min}} \times \frac{300\ \mathrm{K}}{9000\ \mathrm{K}}\\
&= \mathrm{c}\ \mu\mathrm{g\,Ca/mL} \times 1\ \mathrm{mL/\,min} \times 0.05\\
&\times \frac{1\ \mathrm{mole}}{40\ \mathrm{g\,Ca}} \times 6.02 \times 10^{23}/\mathrm{mole}
\end{aligned}$$

$$\times \frac{1}{1000\,\mathrm{cm}^{-3}\,\mathrm{Ar/\,min}} \times \frac{1}{30}$$
$$= \mathrm{c} \times 10^{-6}\,\mathrm{g\,Ca/mL}$$
$$\times\ 1\,\mathrm{mL/\,min} \times 0.05 \times \frac{1\,\mathrm{mole}}{40\,\mathrm{g\,Ca}} \times 6.02 \times 10^{23}/\mathrm{mole}$$
$$\times \frac{1}{1000\,\mathrm{cm}^{-3}\mathrm{Ar/\,min}} \times \frac{1}{30}$$
$$= 2.51 \times 10^{10}\,\mathrm{c/cm^3\,Ar}$$

The values obtained are shown in Table 2. The degree of ionization for Li and K were calculated using the Saha equation. The values obtained were inexcess of the ground state number densities, implying close to 100% ionization.

For the air-acetylene flame experiments, flow number densities were calculated assuming 4.0 ± 0.1 g/min aspiration rate and 5.7 ± 0.2% nebulization efficiency and 2573 K temperature.

RESULTS AND DISCUSSION

Figures 2–4 show the experimental I'/I curves for the effect of excess Li on Ca atom line and excess Li and K on the Ca, Mg, and Sr ion lines. Figure 4 shows the experimental I'/I curves for the effects of Na on K and K on Mg line emission in the air-acetylene flame. The curves in both figures show a sharp increase in line emission signal enhancement with decrease in the concentration of the analyte in the test solution below about 0.5 mg/L. The similarity between the curves for the ICP and flame experiments suggests that the effects of EIEs are due entirely to the presence of the interferent; that is, the differences in the temperature and composition of the ICP and that of the air-acetylene are not significant as far as emission signal enhancement is concerned.

Table 3 shows that $n_{(\mathrm{Ar+})} >> n_{(\mathrm{A+})} + n_{(\mathrm{m+})}$, suggesting that the ICP is dominated by electrons from the ionization of Ar. The noninvolvement of Ar in the signal enhancement means that electronic collisions cannot be the major source of the signal enhancement. The signal enhancement can only be explained on the basis of collisional charge transfer between analyte and interferent species to yield the excited atoms or ions. Taking the effect of excess Li on Ca atom line as an example, in the presence of the interferent, the excitation and de-excitation of Ca might be envisaged to occur according to the steps shown in Table 4.

The mechanism of collisional charge transfer between analyte and interferent was discussed previously.[21,24,25]

Table 2. Flow number densities: ICP experiments and values of M^+/M (experimental at 1 kW radio frequency power) and M^{2+}/M^+ (theoretical at 9000 K) for Mg, Ca, and Sr

	Flow number densities (atoms/ions cm^{-3} s^{-1})						
M	[MI]	(Desig)	[MII]	(Desig)	$n_{(a2+)}$	M^+/M^a (%)	M^{2+}/M^{+b} (%)
Ca	2.5104×10^{10}c	$n_{(a)}$	2.4600×10^{10}c	$n_{(a+)}$	1.5818×10^{9}c	98.90	6.43
Mg	4.1004×10^{10}c	$n_{(a)}$	3.8134×10^{10}c	$n_{(a+)}$	6.8641×10^{7}c	93.00	0.174
Sr	1.1377×10^{10}c	$n_{(a)}$	1.1309×10^{10}c	$n_{(a+)}$	2.2301×10^{9}c	99.40	19.72
Ar	2.6883×10^{19}	$n_{(Ar)}$	2.9242×10^{16}	$n_{(Ar+)}$			
Li	1.4367×10^{14}	$n_{(m)}$	1.4367×10^{14}	$n_{(m+)}$			
K	2.5495×10^{13}	$n_{(m)}$	2.5495×10^{13}	$n_{(m+)}$			

M, element; Desig, designation; c, analyte concentration in mg/L.

Source: [a]Ref. [1]; [b]Ref. [24].

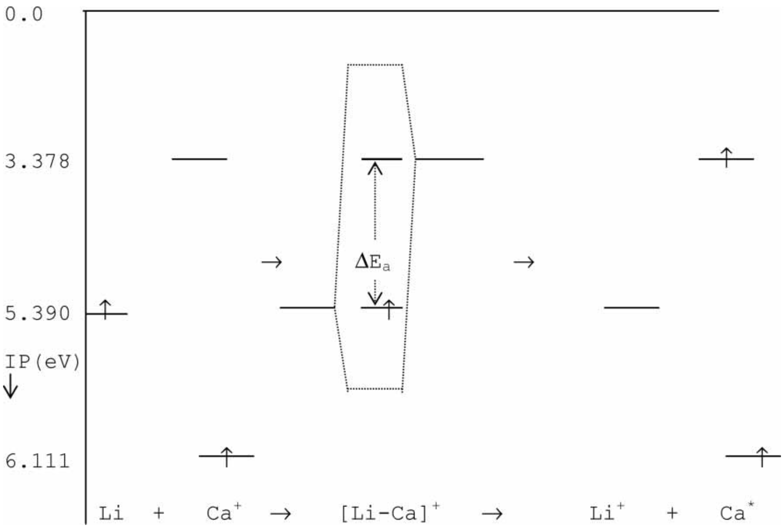

Figure 5. Possible mechanism of collisional charge transfer between the Li atom and Ca^+ ion to give Ca^* excited state.

A possible mechanism for the collisional charge transfer between Li atoms and Ca^+ ions is shown in Fig. 5. In actual practice, charge transfer can be envisaged to proceed with activation of the Li atoms prior to collision.

Assuming a steady state with respect to analyte excited state and the ionic state, we have:

$$d[\mathrm{Ca}^*]/dt = 0 = k_\Delta[\mathrm{Ca}] + k_\#[\mathrm{Ca}^-][\mathrm{Ca}^\#] + k_2[\mathrm{Li}][\mathrm{Ca}^+] - k_{-2}[\mathrm{Ca}^*][\mathrm{Li}^+] - k_{h\nu}[\mathrm{Ca}^*].$$

Table 3. Number densities: air-acetylene experiments

	Flow number densities (atoms/ions cm^{-3} s^{-1})					
M	[MI] cm^{-3}	(Desig)	[MII] cm^{-3}	(Desig)	α	β
K	1.7808×10^{11}c	$n_{(a)}$	1.9589×10^{9}c	$n_{(a+)}$	0.011	
Mg	2.4058×10^{11}c	$n_{(a)}$	1.2029×10^{9}c	$n_{(a+)}$	0.005	84%
Na	3.0287×10^{14}	$n_{(m)}$	2.8167×10^{13}	$n_{(m+)}$	0.093	
K	1.7808×10^{14}	$n_{(m)}$	1.9589×10^{12}	$n_{(m+)}$	0.011	

M, element; Desig, designation; α, degree of ionization[25]; β, atomization efficiency[26]; c, analyte concentration in mg/L.

Table 4. Possible charge transfer steps leading to excitation and/or ionization of Ca in the ICP

Process*		Slow/fast	Rate const.
(i)	$Ca \rightarrow Ca^*$	Slow	k_Δ
(ii)	$Li + Ca^+ \rightarrow Li^+ + Ca^*$	Fast	k_2
(iii)	$Ca^+ + Ca^\# \rightarrow Ca^* + Ca^+$	Fast	$k_\#$
(iv)	$Ca^* + Li^+ \rightarrow Ca^+ + Li$	Fast	k_{-2}
(v)	$Ca^* \rightarrow Ca + h\nu$	$k_{h\nu}$	

*and # denote excitation states of analyte .

Therefore

$$[Ca^*]' = \frac{k_\Delta[Ca] + k_\#[Ca^+][Ca^\#] + k_2[Li][Ca^+]}{k_{h\nu} + k_{-2}[Li^+]} \tag{3}$$

where the prime denotes presence of interferent. In the absence of interferent,

$$[Ca*] = \frac{k_\Delta[Ca] + k_\#[Ca^+][Ca^\#]}{k_{h\nu}} \tag{4}$$

Dividing Eq. (3) by Eq. (4),

$$\frac{[Ca^*]'}{[Ca^*]} = \left\{1 + \frac{k_2[Li][Ca^+]}{k_\Delta[Ca] + k_\#[Ca^+][Ca^\#]}\right\}\left\{\frac{k_{h\nu}}{k_{h\nu} + k_{-2}[Li^+]}\right\}. \tag{5}$$

The rate of collisional charge transfer is derived from collision theory and is given by

$$k_2[Li][Ca^+] = k_c[Li][Ca^+]\exp(-\Delta E_a/kT), \tag{6}$$

where $k_c = \pi d_{12}^2\ (8kT/\pi\mu)^{1/2}$, the collisional rate constant,[27] ΔE_a, is the activation energy, d_{12} is the mean diameter of the colliding species, and μ is the reduced mass.

Current collision theory is arrived at assuming elastic collisions and reflects the fact that in elastic collisions, a particle is capable of multiple collisions, hence the number of collisions is proportional to the product of the concentrations or number densities of the colliding particles. In inelastic collisions, each such collision results in a reaction. Thus for a closed system, the concentration of reactant in lower concentration will determine the extent of reaction. For flow systems, it will be the concentration of the reactant in higher concentration that determines the extent or rate of reaction. In other words, the rate of collisions cannot be higher than the rate at which the reactant in higher concentration is introduced into the plasma.

Taking these rates (in Table 5) into account, Eq. (5) can be generalized to

$$\frac{n'_u}{n_u} = \left[1 + \frac{n_{(m)}}{k_\Delta n_{(a)} + (1-\alpha)n_{(a)}}\right]\left[\frac{k_{h\nu}}{k_{h\nu} + n_{(m^+)}}\right]. \tag{7}$$

By assuming $(n_{(a)}/k_\Delta n_{(a)}) >> 1$ and making appropriate substitution, it can be shown that Eq. (7) converts to Eq. (8), thus:

$$\frac{n'_u}{n_u} = 1 + \left[\frac{n_{(m)}}{k_\Delta n_{(a)} + (1-\alpha)n_{(a)}}\right]\left[\frac{k_{h\nu}}{k_{h\nu} + n_{(m^+)}}\right]. \tag{8}$$

After substituting the appropriate values from Tables 3 and 5, we arrive at Eq. (9) for the effects of 1000 mg/L Li on the Ca atom line:

$$(n'_u/n_u)_{\mathrm{CaI/Li}} = 1 + 4.4405 \times 10^{-1}/c, \tag{9}$$

where c is analyte concentration.

For the Ca ion line, assuming $[\mathrm{Ca}^{\#}] >> [\mathrm{Ca}^{2+}]$, where $\mathrm{Ca}^{\#}$ represents all species derived from Ca other than Ca^{2+} ions, gives

$$\frac{n'_u}{n_u} = 1 + \left[\frac{n_{(m)}}{k_\Delta n_{(a)} + n_{(a^{2+})}}\right]\left[\frac{k_{h\nu}}{k_{h\nu} + n_{(m^+)}}\right], \tag{10}$$

where $n_{(a2+)} = [\mathrm{Ca}^{2+}]$

For the effects of 1000 mg/L Li or K on Ca, Mg, and Sr ion lines:

$$(n'_u/n_u)_{\mathrm{CaII/M}} = 1 + 2.7246 \times 10^{-1}/c \tag{11}$$

$$(n'_u/n_u)_{\mathrm{MgII/M}} = 1 + 3.1564 \times 10^{-1}/c \tag{12}$$

$$(n'_u/n_u)_{\mathrm{SrII/M}} = 1 + 1.4968 \times 10^{-1}/c, \tag{13}$$

where the subscript M denotes interferent element, in this case Li or K.

For systems in the air-acetylene flame, $[\mathrm{Ca}^{\#}] >> [\mathrm{Ca}^{+}]$ because of the low degree of ionization of the analyte at the low flame temperature. In addition, analytes are only ionized to a very low extent in the air-acetylene. Easily ionized elements enhance analyte ionization, as well as excitation,

Table 5. Rates calculated for processes in Eq. (4)

Process	Rate equation	Value (s^{-1})
k_Δ [Ca]	$[\mathrm{Ca}]g_u/g_o \exp(-2.933\ \mathrm{eV}/kT)$	8.4479×10^8c
k_2 [Li] $[\mathrm{Ca}^+]$	$k_c[\mathrm{Li}]\ [\mathrm{Ca}^+] \exp(-2.022\ \mathrm{eV}/kT)$	3.6178×10^{14}c
$k^{\#}$ $[\mathrm{Ca}^+][\mathrm{Ca}^{\#}]$	$\alpha(1-\alpha)\ k_c[\mathrm{Ca}]^2$	$1.3799 \times 10^{10}c^2$
k_{-2} $[\mathrm{Ca}^*]$ $[\mathrm{Li}^+]$	$k_c[\mathrm{Li}^+]\ [\mathrm{Ca}]g_u/g_o \exp(-2.933/kT)$	5.1571×10^{14}c
$k_{h\nu}n_u$	$k_{h\nu}[\mathrm{Ca}]g_u/g_o.\exp(-2.933\ \mathrm{eV}/kT)$	3.1521×10^{17}c

*Analyte/interferent; α, degree of ionization; c, analyte concentration in mg/L; # all species derived from analyte (M) other than M^{2+} ions.

Table 6. Rates of limiting steps for processes in Eq. (4)

Process	Rate of limiting step	Values for Ca(I)/Li* system
$k_{\Delta}[\mathrm{Ca}]$	$k_{\Delta}[\mathrm{Ca}]\ \mathrm{s}^{-1}$	$8.4479 \times 10^{8}c$
$k_2[\mathrm{Li}]\ [\mathrm{Ca}^{+}]$	$n_{(\mathrm{Li})}\ \mathrm{s}^{-1}$	1.4367×10^{14}
$k^{\#}[\mathrm{Ca}^{+}]\ [\mathrm{Ca}^{\#}]$	$[\mathrm{Ca}^{\#}] = (1-\alpha)n_{(\mathrm{Ca})}\ \mathrm{s}^{-1}$	$2.7361 \times 10^{8}c$
$k_{-2}[\mathrm{Ca}^{*}]\ [\mathrm{Li}^{+}]$	$n_{(\mathrm{Li+})}\ \mathrm{s}^{-1}$	1.4367×10^{14}
$k_{h\nu}n_{\mathrm{u}}$	$k_{h\nu}$	3.7312×10^{8}

*Analyte/Interferent; α, degree of ionization.

through charge transfer as follows:

$$\text{(i)}\quad \mathrm{K}^{+} + \mathrm{Mg} \rightarrow \mathrm{Mg}^{+} + \mathrm{K}$$

$$\text{(ii)}\quad \mathrm{K} + \mathrm{Mg}^{+} \rightarrow \mathrm{Mg}^{*} + \mathrm{K}^{+}.$$

The rate-determining step is (i), hence Eq. (5) becomes

$$\frac{n'_u}{n_u} = 1 + \left[\frac{n_{(m^{+})}}{k_{\Delta}n_{(a)} + n_{(a^{+})}}\right]\left[\frac{k_{h\nu}}{k_{h\nu} + n_{(m^{+})}}\right] \tag{14}$$

After making the appropriate substitutions, we arrive at Eqs. (15) and (16) for the effects of 1000 mg/L Na on the K atom line, and 1000 mg/L K on Mg atom line in the air-acetylene flame:

$$(n'_{\mathrm{u}}/n_{\mathrm{u}})_{\mathrm{K/Na}} = 1 + 5.793 \times 10^{-2}/c \tag{15}$$

$$(n'_{\mathrm{u}}/n_{\mathrm{u}})_{\mathrm{MgI/K}} = 1 + 6.8139 \times 10^{-1}/c \tag{16}$$

If we assume $I'/I = n_{\mathrm{u}}'/n_{\mathrm{u}}$, then the calibration curve in the presence of excess easily ionized element can be predicted from the appropriate $n_{\mathrm{u}}'/n_{\mathrm{u}}$ equation and line emission readings in the absence of the interferent, according to Eq. (17):

$$I' = I(n'_{\mathrm{u}}/n_{\mathrm{u}}). \tag{17}$$

Figure 2 shows the $n_{\mathrm{u}}'/n_{\mathrm{u}}$, experimental and predicted calibration curves for the Ca atom and ion lines in the presence of 1000 mg/L Li as interferent in the ICP. It is apparent from Fig. 2 that very good agreement between theory and experiment is obtained. Figure 3 shows the $n_{\mathrm{u}}'/n_{\mathrm{u}}$ curves and predicted calibration curves for the Mg and Sr ion lines in the presence of 1000 mg/L Li as interferent, and Fig. 4 shows the $n_{\mathrm{u}}'/n_{\mathrm{u}}$ curves and predicted calibration curves for the Mg and Sr ion lines in the presence of 1000 mg/L K as interferent in the ICP. The experimental curves are included for comparison. It is apparent from Figs. 3 and 4 that extremely good agreement between theory and experiment is obtained ($\mathrm{R}^2 = 0.99789$). The small deviations from a straight line obtained for all calibration curves could be explained by the possibility of contamination of the interferent salts. For example, a typical AR grade LiCl salt (which contains about 0.005% Ca) in 1000 mg/L Li solution gives 0.05 mg/L Ca contamination. However, the general shapes of the theoretical and experimental curves remain similar in all experiments.

Figures 5A and 5B show the n_u'/n_u curves and predicted calibration curves for the K atom line in the presence of 1000 mg/L Na as interferent, and Figs. 5C and 5D show the n_u'/n_u curves and predicted calibration curves for the Mg atom line in the presence of 1000 mg/L K as interferent in the air-acetylene flame. Again, the experimental curves are included for comparison. It is apparent from Fig. 5 that very good agreement between theory and experiment is obtained.

The possibility of charge transfer processes contributing to excitation mechanisms in the ICP was discussed by several workers. Penning ionization involving Ar metastable states has been suggested as one process whereby analyte atoms might be ionized or excited,[28] the other being charge transfer involving Argon ions.[29,30] The similarity between the I'/I curves for the flame and ICP experiments reported in this paper would tend to suggest that the effect of charge transfer processes involving Ar species on analyte excitation is negligible under the experimental conditions employed for the ICP.

Direct charge transfer between analyte and interferent has also been suggested for systems in the air-acetylene flame,[20,21,33] whereby the interferent catalyzed the ionization of analyte atoms for subsequent excitation via radiative recombination. The current work suggests that direct analyte excitation via collisional charge transfer with activated interferent atoms is possible.

Examination of Eq. (8) shows that when $n_{(m+)} >> k_{h\nu}$, Eq. (8) reduces to

$$\frac{n_u'}{n_u} = 1 + \left[\frac{k_{h\nu}}{k_{\Delta}n_{(a)} + (1-\alpha)n_{(a)}}\right]\left[\frac{n_{(m)}}{n_{(m^+)}}\right], \tag{18}$$

that is, the observed emission signal enhancement is an inverse function of the degree of ionization of the interferent. This is in agreement with the finding by Henselman et al.[31] after a study of the effect of sample matrix on electron density and electron temperature in the ICP using Thompson and Rayleigh scattering; in general, the order of n_e and T_e enhancement is an inverse function of the ionization potential of the interferent. The degree of ionization is a very sensitive function of temperature and may explain in part the spatial variation of emission signal enhancement due to easily ionized elements that has been widely reported.[2,29]

Interference effects from easily ionized element matrices in the ICP were reviewed by Blades and Horlick.[2] These workers concluded that the exact nature of the interference with the analyte emission is complex. Examination of the calibration curves in Figs. 2 to 5 confirms this. For example, although very good agreement is obtained between experiment and theory for the effect of Li or K on Mg and Sr ion lines, the calibration curves obtained in each case for Mg and Sr exhibit differences that point to the existence of analyte-specific factors not readily explainable from this limited work. The same applies to the calibration curves for the effect of Li on Ca atom and ion lines (Fig. 2).

CONCLUSIONS

The results presented in this paper show that the effect of easily ionized elements during ICP-AES and flame AES can be described using a simplified rate model based on collisional charge transfer between analyte and interferent species for analyte concentration spanning the 0–10 mg/L range. Theoretical calibration curves derived based on the simplified model showed a good agreement with experimental curves. However, we should point out that the simplified rate model as presented in this paper may not tell the full story as far as mechanisms of excitation in flame AES or ICP-OES are concerned, but the fact that it leads to close simulation of the analytical calibration curve obtained in the presence of easily ionized interferents is of significance.

ACKNOWLEDGMENTS

This work was supported by a grant from the Research Board of the University of Zimbabwe (UZ). The courtesy of the director and staff of the Institute of Mining Research of UZ, Mr. Kahwai and Mr. Ansari, and that of the management and staff of Bindura Nickel Corporation in availing us the use of their ICP spectrophotometers is gratefully acknowledged.

REFERENCES

1. Blades, M. W. *Inductively Coupled Plasma Emission Spectrometry*; Boumanns, P. W. J. M., Ed.; Wiley Interscience: New York, 1987; p. 387, Part, II.
2. Blades, M. M. W.; Horlick, G. *Spectrochim. Acta* **1981**, *36B* (9), 881–900.
3. Olivares, J. A.; Houk, R. S. *Anal. Chem.* **1986**, *58*, 20.
4. Gregoire, D. C. *Spectrochim. Acta* **1987**, *42B* (7), 895–907.
5. Rayson, G. D.; Hieftje, G. M. *Spectrochim. Acta* **1986**, *41B* (7), 683–697.
6. Boumans, P. W. J. M.; DeBoer, F. J. *Spectrochim. Acta* **1976**, *31B*, 355.
7. Boumans, P. W. J. M. *Spectrochim. Acta* **1982**, *37B*, 75.
8. Uchida, H.; Tanabe, K.; Nojiri, Y.; Haraguchi, H.; Fuwa, K. *Spectrochim. Acta* **1980**, *35B*, 881.
9. Poluektov, N. S.; Vitkum, R. A. *Zhur Anal. Khim* **1961**, *16*, 260.
10. Smit, J.; Alkemade, C. T. J.; Verschure, J. C. M. *Biochim. Biophys. Acta* **1951**, *6*, 508.
11. Brockaert, J. A. C.; Leis, F.; Laqua, K. *Spectrochim. Acta* **1979**, *34B*, 167.

12. Van der Mullen, J. A. M.; Raaijmakers, I. K. M. M.; van Lammeren, A. C. A. P.; Schram, D. C.; van der Sijde, B.; Schenkelaars, H. J. W. *Spectrochim. Acta* **1987**, *42B*, 1039–1051.
13. Blades, M. W. *Spectrochim. Acta* **1982**, *37B*, 869.
14. Blades, M. W.; Hieftje, G. M. *Spectrochim. Acta* **1982**, *37B*, 191.
15. Mills, J. W.; Hieftje, G. M. *Spectrochim. Acta* **1984**, *39B*, 859.
16. Alder, J. F.; Bombelka, R. M.; Kirkbright, G. F. *Spectrochim. Acta* **1980**, *39B*, 163.
17. Lovett, R. J. *Spectrochim. Acta* **1982**, *37B*, 969.
18. Eljoundi, A.; Batal, A.; Mermert, J. M. *Spectrochim. Acta* **1985**, *40B*, 1007.
19. George, C.-Y.; Chan; Wing-Tat Chan; Xianglei Mao; Russo, R. E. *Spectrochim. Acta* **2000**, *55B*, 221–235.
20. George, C-Y.; Chan; Wing-Tat Chan; Xianglei Mao; Russo, R. E. *Spectrochim. Acta* **2001**, *56B*, 77–92.
21. Zaranyika, M. F.; Chirenje, A. *Fresenius J. Anal. Chem.* **1999**, *364*, 208–214.
22. Zaranyika, M. F.; Nyakonda, C.; Moses, P. *Fresenius. J. Anal. Chem.* **1991**, *341*, 577–585.
23. Unicam Ltd (Division of Analytical Technology Inc.). Unicam 701 Series, I.C.P Systems Operating Manual, Issue 1 (10/92). Unicam Ltd: Cambridge, UK, 1992.
24. Rohatgi-Mukherjee, K. K. *Fundamentals of Photochemistry*; Wiley: New York, 1978; p. 7.
25. Pupyshev, A. A.; Semenova, E. V. *Spectrochim. Acta* **2001**, *56B*, 2397–2418.
26. Willard, H. H.; Merritt, L. L.; Dean, J. A.; Settle, Fa., Jr. *Instrumental Methods of Analysis*, 7th edn.; Wadsworth: Belmont, CT, 1988; p. 232.
27. Winefordner, J. D.; Schulman, S. G.; O'Haver, T. C. *Luminescence Spectrometry in Analytical Chemistry*; Wiley-Interscience: New York, 1972.
28. Horner, J. A.; Hieftje, G. M. *Spectrochim. Acta* **1996**, *53B*, 1235–1259.
29. Goldwasser, A.; Mermert, J. M. *Spectrochim. Acta* **1986**, *41B*, 725.
30. Raaijmakers, I. K. M. M.; Schram, D. C.; Boumans, P. W. J.; van der Sijde, B.; Schenkelaars, H. J. W. *Spectrochim. Acta* **1983**, *38B*, 1545.
31. Raaijmakers, I. K. M. M.; Boumans, P. W.J.; van der Sijde, B.; Schram, D. C. *Spectrochim. Acta* **1983**, *38B*, 697.
32. Hanselman, D. S.; Sesi, N. N.; Huang, M.; Hieftje. *Spectrochim. Acta* **1994**, *49B*, 495–526.
33. Allen, C. W. *Astrophysical Quantities*; Athrone Press: London, 1955.